

# 3-D Microscopy Tomography under Sparsity Constraint

Jinwook Jung, Jaeduck Jang, Hyosang Kim, Jong Chul Ye

KAIST/Department of BioSystems, Daejeon, Republic of Korea

**Abstract**—There has been considerable research interest in reconstructing three-dimensional structure of biological cells using microscope. Off-axis illumination system is generally used for low or middle magnification, but many numbers of projections are usually required for good image reconstruction. This paper proposes a new algorithm such that three-dimensional sample can be reconstructed using only a few projection if the cells are distributed sparsely along phantom.

**Keywords**— microscopy tomography, reconstruction, sparsity

## I. INTRODUCTION

Three-dimensional reconstruction using wide field optical microscope is divided into two branches, one for low and middle magnification, and the other for high magnification. For higher magnification, z-stacks are obtained and deconvolution is used for 3-D reconstruction. However, for low or middle magnification, off-axis illumination system using off-centered aperture is more preferable [1]. In this paper, low and middle magnification microscope is considered for micro fluidic chip monitoring. Generally, many numbers of projections are required for best image quality in a rotationally off-axis illumination system [1]. However, we propose a new reconstruction method which allows accurate reconstruction using only small number of projections.

In chapter II, 10 x optical microscopes is designed using optical design software (ZEMAX<sup>®</sup>), and PSF data is obtained from the designed microscope. We suggest the PSF interpolation method and verify the algorithm in chapter III. Using these PSF data, we propose a new reconstruction algorithm in chapter IV. The simulation results show excellent 3-D reconstruction using even with 4 projections.

## II. MICROSCOPE DESIGN FOR 3-D IMAGING

3D microscope imaging can be done by placing an off axis stop between lens and detector as depicted in Fig. 1(a). As seen from Fig. 1(b), the rotating off-axis stop measurements provide tilted view images similar to those of rotating samples in the image plane. Therefore, by

processing the data obtained from rotating the off-axis stop using appropriate algorithm, the three-dimensional information about samples can be obtained.

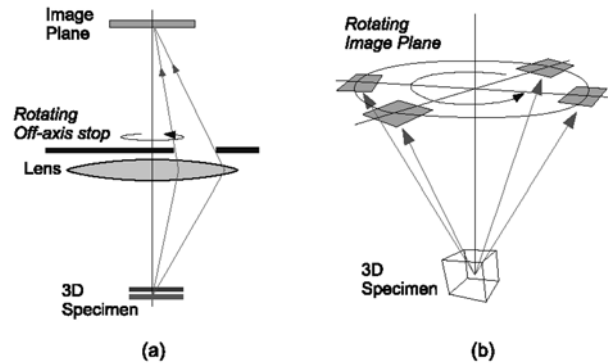


Fig. 1 Sketch of 3-D microscope tomography

The ZEMAX software has been used for design and optimization of microscope. The design for proposed 3-D microscope is shown in Fig. 2

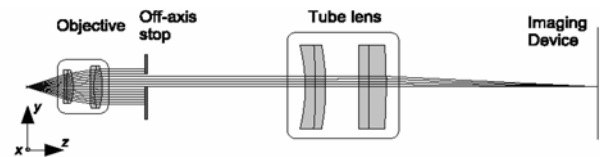


Fig. 2 Outline for 3D microscope

Fig. 3 shows the structure of microscope and the parameters which are used for simulation. Objective lens is composed of two doublet lens, and it has 10 magnifications, 11mm working distance, 18mm focal distance, 0.25 NA. Tube lens is also composed of two doublets, and its focal distance is 180mm. The total magnification of microscope is around 10.

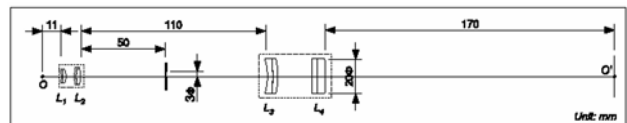


Fig. 3 Design for 3D microscope

Figure 3 shows that the stop is placed between the objective lens and tube lens. The distance between the objective lens and stop affects the field of view, and in this design the distance was fixed at 60mm in which we presume that one or two optical components can be inserted. Also, the stop diameter and the distance from optical axis were fixed 3mm and 1.5mm respectively.

### III. PSF INTERPOLATION

For efficient 3-D image reconstruction using microscope, information about PSFs (Point Spread Function) is needed. The PSF data can be calculated or measured; however, it is too time-consuming to get the PSFs for every image voxel. So, a few PS measurements around 50~100 are obtained, and other PSFs are calculated using interpolation method.

Because the tendency of PSF variation is very complicated, it is required to consider another physical value, which is suitable for interpolation. OTF (Optical Transfer Function) is Fourier pair of PSF, and its center value is always 1. Also, PSF has ring-shaped side lobe and null affected by limited size and boundary of stop, whereas OTF gradually decreases to 0 from the center. Hence, we propose to use OTF for interpolating PSF values. The detailed algorithm is as following:

#### A. Interpolation Algorithm

##### 1) Data preprocessing

1. Determine the field of view of the samples. In this paper,  $600 \times 600 \times 100 (\mu\text{m}^3)$  centered on a focal point is assumed.
2. Measure PSF at finite number of nodes in the FOV.
3. Determine the center of PSF  $(x_0, y_0)$  for each node.
4. Compute OTF for each node.

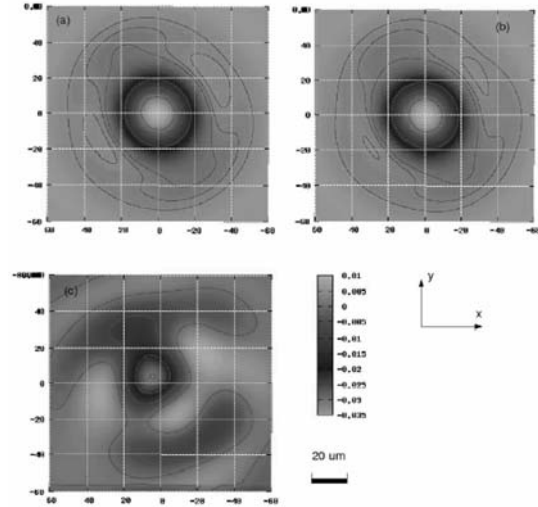
##### 2) PSF Interpolation

1. For the field to calculate the PSF, find the adjacent nodes with calculated (or measured) PSF values.
2. Compute the center of PSF using interpolation from the adjacent data.
3. Interpolate the OTF using OTF data from adjacent neighbors.
4. Calculate the PSF from OTF using FFT(Fast Fourier Transform)  
Save PSF center position and OTF values.

#### B. Verification of interpolation algorithm

To verify the proposed interpolation algorithm, the interpolated PSF is compared with the one obtained from

ZEMAX software for specific field position. Figs. 4(a), (b) show the PSF from simulation and PSF from interpolation for field position  $(0.25, 0.25, -0.04)$  respectively. The adjacent 8 nodes with measured PSF are a:(0.2, 0.2, -0.05), b:(0.3, 0.2, -0.05), c:(0.3, 0.3, -0.05), d:(0.2, 0.3, -0.05), e:(0.2, 0.2, -0.025), f:(0.3, 0.2, -0.025), g:(0.3, 0.3, -0.025), h:(0.2, 0.3, -0.025). Each PSF is normalized to have the maximum value 1. A difference between two un-normalized PSFs is presented in the Fig. 4(c). The maximum difference is 0.03, that is, very small error.



(a) PSF from simulation (b) PSF from interpolation (c) difference

Fig. 4 PSF from ZEMAX versus PSF from Interpolation

### IV. RECONSTRUCTION ALGORITHM

In microscope tomography system, the relationship between measured image on the CCD cameras and subject image on the microscopy can be simplified as a linear form:

$$\mathbf{P} = [p^{1T} \ \cdots \ p^{VT}]^T = [\mathbf{A}^1 \ \cdots \ \mathbf{A}^V]^T \mathbf{f}, \quad (1)$$

where  $p \in \mathbf{R}^{N^2 \times 1}$ ,  $\mathbf{A} \in \mathbf{R}^{N^2 \times (M^2 \times n)}$ , and  $\mathbf{f} \in \mathbf{R}^{(M^2 \times n) \times 1}$  denotes the CCD screen measurement, the discretized PSF function, and 3-D sample volume, respectively. Here,  $N^2$  denotes the number of CCD camera pixel, and the number of voxel for each layer is  $M^2$ ; and  $V$  and  $n$  denote the number of CCD camera view and reconstructed volume layer in microscopy system, respectively. To solve this problem, we define the cost function in a Bayesian framework by computing maximum *a posteriori* (MAP) estimate for  $\mathbf{f}$  given observation  $\mathbf{y}$ . The MAP estimate is

then the value of  $\hat{\mathbf{f}}$  which minimizes the *a posteriori* density given the observations  $\mathbf{P}$  [3]:

$$\begin{aligned}\hat{\mathbf{f}} &= \arg \max_{\mathbf{f}} L_p(\mathbf{f} | \mathbf{y}) \\ &= \arg \max_{\mathbf{f}} \{L(\mathbf{y} | \mathbf{f}) + \log G(\mathbf{f})\}.\end{aligned}\quad (2)$$

We can derive the approximation [3]

$$L(\mathbf{y} | \mathbf{f}) = -\frac{1}{2\sigma^2} \sum_{\alpha=1}^V \|\mathbf{P}^\alpha - \mathbf{A}^\alpha \mathbf{f}\|^2, \quad (3)$$

The Gaussian Markov random field (GMRF) is widely adapted in many image reconstruction problems [4]. For the prior distribution, the GMRF uses the log probability density function with the quadratic form

$$\log G(\mathbf{f}) = -\frac{\gamma}{2} \mathbf{f}^T \mathbf{R} \mathbf{f} + c, \quad (4)$$

where  $(1/\gamma)\mathbf{R}^{-1}$  is the covariance matrix. In particular,  $\mathbf{R}$  reflects the correlation structure of spatially adjacent pixels. Therefore MAP estimation is written as follow

$$\begin{aligned}\hat{\mathbf{f}} &= \arg \max_{\mathbf{f}} L(\mathbf{f} | \mathbf{y}) \\ &= \arg \max_{\mathbf{f}} \left\{ \frac{1}{2\sigma^2} \sum_{\alpha=1}^V \|\mathbf{P}^\alpha - \mathbf{A}^\alpha \mathbf{f}\|^2 + \frac{\gamma}{2} \mathbf{f}^T \mathbf{R} \mathbf{f} \right\},\end{aligned}\quad (5)$$

Changing the value of  $\mathbf{f}$  at the point  $i$  by the amount  $\Delta \mathbf{f}_i$ , results in the changes of the projection error in the following way:

$$\hat{e}^\alpha = e^\alpha - \mathbf{A}_{*i}^\alpha \Delta \mathbf{f}_i, \quad \alpha = 1, \dots, V \quad (6)$$

where  $\mathbf{A}_{*i}^\alpha$  is the  $i$ th column of  $\mathbf{A}^\alpha$  and  $\hat{e}^\alpha$  is the  $\alpha$ th view of the new value of the projected error. The equation for the new log likelihood is

$$\begin{aligned}L(\mathbf{y} | \hat{\mathbf{f}}) &= -\frac{1}{2\sigma^2} \sum_{\alpha=1}^V \|\mathbf{P}^\alpha - \mathbf{A}^\alpha \hat{\mathbf{f}}\|^2 \\ &= L(\mathbf{y} | \mathbf{f}) + \theta_1 \Delta \mathbf{f}_i - \frac{1}{2} \theta_2 (\Delta \mathbf{f}_i)^2,\end{aligned}\quad (7)$$

where  $\hat{\mathbf{f}}_i = \mathbf{f}_i + \Delta \mathbf{f}_i$ . The values  $\theta_1$  and  $\theta_2$  are defined by

$$\theta_1 = \frac{1}{\sigma^2} \sum_{\alpha=1}^V \mathbf{A}_{*i}^{\alpha T} e^\alpha, \quad (8)$$

$$\theta_2 = \frac{1}{\sigma^2} \sum_{\alpha=1}^V \mathbf{A}_{*i}^{\alpha T} \mathbf{A}_{*i}^\alpha. \quad (9)$$

For update each pixel, Eqs. (8) and (9) plays important role. From the definition of Eq. (8),  $\theta_1$  corresponds to the pixel-driven backprojection [6] of residual images on the

CCD screen for the  $i$ th pixel. Similarly,  $\theta_2$  corresponds to the energy of the PSF function at the  $i$ th voxel. Hence, instead of storing  $\mathbf{A}^\alpha$  matrix, we need to save PSF image of each voxel location for each view, which greatly saves the memory requirement. Indeed, if the optical system is ideal, the PSF function is stationary; we only need to save  $V$  number of PSF image. Let  $S$  denote the number of non-zero pixel of PSF images. Since the optical microscope tomography, the PSF has small support  $S \ll N^2$  due to the small NA value; hence the memory requirement is small. If we use Gaussian prior distribution, the optimum value for  $\Delta \mathbf{f}_i$  is given by

$$\Delta \mathbf{f}_i = \frac{\theta_1 - \eta \mathbf{R}_{*i} \mathbf{f}}{\theta_2 + \eta \mathbf{R}_{*i}}, \quad (10)$$

where  $\eta = \gamma \sigma^2$ . The total update equations for each pixel are Eqs. (8), (9), and (10). In the case of Eq. (9), it can be pre-calculated before reconstruction process.

## V. EXPERIMENT RESULT

We have performed extensive computer simulations with synthetic data to illustrate reconstruction performance of the proposed algorithm. Instead of 3-D volume subject, multiple layers images with  $64^2 \times n$  square elements are used for forward and inverse solvers. The measured images with  $512^2 \times V$  square elements are multiple aperture angles of CCD camera. As mentioned earlier,  $n$  and  $V$  are equal to the sample layers and the number of CCD camera view, respectively. We have 4 aperture angle (e.g.  $0^\circ$ ,  $90^\circ$ ,  $180^\circ$ ,  $270^\circ$ ) for CCD camera view ( $V=4$ ) and various number of subject image layers. For simplicity,  $\mathbf{R}$  in GMRF is defined as

$$r_{(i,j)} = \begin{cases} 1 & \text{if } i = j; \\ \frac{1}{4} & \text{if } |i - j| = 1; \\ 0 & \text{otherwise.} \end{cases} \quad (15)$$

It means that we choose eight-point neighborhood system considering vertical and horizontal pixels with weighting factor ( $1/4$ ). Additionally,  $\eta = \gamma \sigma^2$  determines the tradeoff between sharpness and noise level; so it is chosen by trade-off for a given geometry and used for consequent simulation with the same geometry. To compare the reconstruction performance, we used 2 volume data, which consist of various layers.

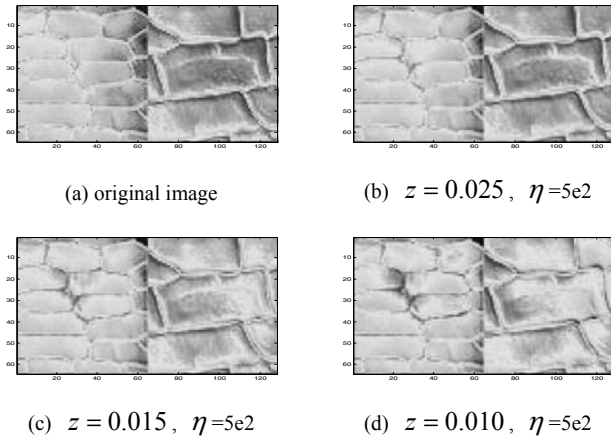


Fig. 5 The reconstructed skin images ( $n = 2$ )

In order to compare the reconstruction results, skin images and cell images with two layers are reconstructed with difference layer depth ( $z$ ). As shown in Fig. 5, layer depth contributes to the reconstruction images.

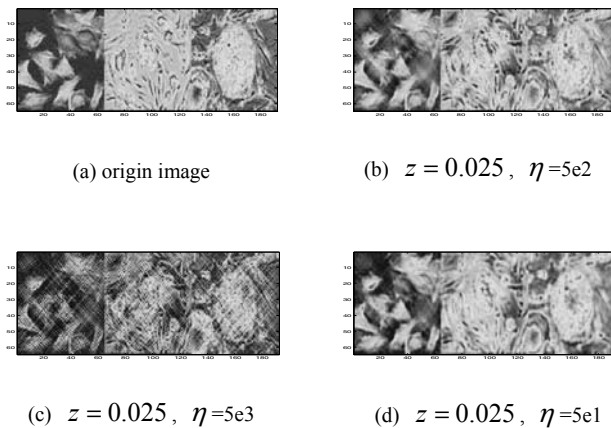


Fig. 6 The reconstructed cell images ( $n = 3$ )

The cell image with three layers is reconstructed with different  $\eta$ . The smallest  $\eta$  in Fig. 6 shows the notable edges in the reconstructed image. Conversely, the biggest  $\eta$  shows the smoothing effect comparing to Fig. 6(b).

## VI. CONCLUSION

In this paper, we have designed the optical microscopy tomography system using commercial optical software

ZEMAX<sup>®</sup> to analyse and optimize the trade-off of the optical microscope tomography. Furthermore, we have developed a novel PSF interpolation method in order to obtain the inhomogeneous PSF functions from a small set of measured PSFs. The simulation results showed that the interpolated PSF has good accuracy. We also developed ICD based 3-D reconstruction algorithm. Extensive simulation with numerical phantom showed very accurate reconstructions even from very limited number of views. The results in this paper should be understood as an optimised estimation of the optical microscope system performance since the real optical system has very subtle aberration which cannot be explained by numerical simulation. However, the general trend of the real optical microscope system would show the similar behaviour. Currently, we are building the optical tomography systems based on the design, and the results will be reported elsewhere.

## VII. ACKNOWLEDGMENT

The authors would like to thank Dr. Bongwan Lee at Fiberpro inc. for helpful discussion. This work was supported by Ministry of Commerce, Industry and Energy (MOCIE), Korea (grant number: 10017755).

## REFERENCES

1. Kawata S, Nakamura O, and Minami S (1987) Optical microscope tomography. I. Support constraint, J Opt Soc Am A 4 292-.
2. ZEMAX<sup>®</sup> is a product of the Zemax Development Corporation, Bellevue, WA.
3. Van Trees H L (1968) Detection estimation and linear modulation theory, John Wiley and Sons.
4. Chellappa R, and Chatterjee S (1985) Classification of textures using Gaussian Markov random fields, IEEE Trans Acoustics Speech and Signal Processing 33 959-963.
5. Bouman C A and Sauer K (1996) A unified approach to statistical tomography using coordinate descent optimization, IEEE Trans Image Processing 5 480-492.
6. Hsieh J (2003) Computed tomography: Principle, Design, artifacts, and Recent Advances, SPIE Press.

Address of the corresponding author:

Author: Jong Chul Ye  
 Institute: Korea Advanced Inst. of Science & Technology (KAIST)  
 Street: 373-1 Guseong-Dong, Yuseong-Gu 305-701  
 City: Daejeon  
 Country: Korea  
 Email: jong.ye@kaist.ac.kr